

# Reactions of Laser-Ablated Boron Atoms with Methanol. Infrared Spectra and *ab Initio* Calculations of CH<sub>3</sub>BO, CH<sub>2</sub>BOH, and CH<sub>2</sub>BO in Solid Argon

Dominick V. Lanzisera and Lester Andrews\*

Department of Chemistry, University of Virginia, Charlottesville, Virginia 22901

Received: November 11, 1996; In Final Form: December 17, 1996<sup>⊗</sup>

Laser-ablated boron atoms react with methanol to give primarily CH<sub>3</sub>BO, which is isolated in an argon matrix. FTIR spectra of various isotopic combinations and MP2 calculated isotopic frequencies help identify this product and the minor products, CH<sub>2</sub>BOH and CH<sub>2</sub>BO. All new products form via boron insertion into the C–O bond, while HBO and DBO form via boron insertion into the O–H bond; no C–H insertion products can be observed. All of these products contain partial dative B–O bonds in which an oxygen lone pair bonds with the empty boron p-orbital.

## Introduction

In matrix isolation studies of the reactions of boron atoms with ammonia and methylamines, the major products were iminoboranes, compounds isoelectronic with alkynes and containing a B–N triple bond.<sup>1–3</sup> *Ab initio* calculations of these compounds predicted vibrational frequencies close to observed values with linear R–B≡N–R (R = H, CH<sub>3</sub>) geometries for all iminoboranes. In these configurations, then, nitrogen donates its electron pair to a bond between its p-orbital and the otherwise empty boron p-orbital. The electron deficiency of boron determines the structure of these compounds despite the separation of formal charge.

The methylamine experiments also revealed that boron prefers to insert into the C–N and N–H bonds, but not into the C–H bonds.<sup>3</sup> The strength of the C–H bonds, relative to other bonds in the molecule, prevents significant boron insertion into these bonds compared to insertion into C–N and N–H bonds. These experiments served as a bridge between studies of boron reacting with CH<sub>4</sub><sup>4,5</sup> and NH<sub>3</sub>,<sup>1,2</sup> and the main products of the CH<sub>3</sub>NH<sub>2</sub> reactions resembled the products of the NH<sub>3</sub> reactions, but with methyl group substitution.<sup>3</sup>

Analogous to the comparison of boron reactions with ammonia and methylamine are comparisons of boron reactions with water and methanol. Matrix isolation studies of reactions of laser-ablated boron atoms with water revealed that boron inserts into the O–H bond, followed by HBOH decomposition to products such as HBO and BO.<sup>6</sup> In this paper, we report the product spectra of B + CH<sub>3</sub>OH reactions. These reactions resemble the H<sub>2</sub>O reactions, but with one hydrogen atom replaced by a methyl group, as in the transition between NH<sub>3</sub> and CH<sub>3</sub>NH<sub>2</sub> reactions. While insertion into H<sub>2</sub>O must involve an O–H bond, insertion into CH<sub>3</sub>OH can take place in a C–H, C–O, or O–H bond. Discussion of the competing insertion mechanisms will be presented as will a discussion of B–O bonding.

## Experimental Section

Previous articles have described the apparatus for pulsed laser ablation, matrix isolation, and FTIR spectroscopy.<sup>2,7</sup> Mixtures of 1% CH<sub>3</sub>OH in Ar codeposited at 3 mmol/h for 2 h onto a 6–7 K cesium iodide window react with boron atoms ablated from a target source rotating at 1 rpm. The fundamental 1064 nm beam of a Nd:YAG laser (Spectra Physics DCR-11)

operating at 10 Hz and focused with a +10 cm focal length lens ablated the target using 20–30 mJ per 10 ns pulse. Reagent gases included vapor from liquid CH<sub>3</sub>OH (J.T. Baker) and CD<sub>3</sub>OD (Cambridge Isotopes). Because the CD<sub>3</sub>OD experiments followed those using CH<sub>3</sub>OH, the manifold remained passivated with acidic H, and the nominally CD<sub>3</sub>OD experiments contained CD<sub>3</sub>OH impurity. Three samples of boron were used: <sup>nat</sup>B (Aldrich, 80.4% <sup>11</sup>B, 19.6% <sup>10</sup>B), <sup>10</sup>B (93.8%, Eagle Pitcher Industries), and <sup>11</sup>B (97.5%, Eagle Pitcher Industries). Following deposition, a Nicolet 550 Fourier transform infrared (FTIR) spectrometer collected infrared spectra using a liquid nitrogen cooled MCT detector. The resolution of these spectra was 0.5 cm<sup>-1</sup> fwhm with an accuracy of ±0.2 cm<sup>-1</sup>. After sample deposition, annealing to 15 K followed by 45 min of broad-band mercury arc photolysis (Philips 175 W) produced changes in the FTIR spectra. Further annealings to 25 and 35 K also altered some of the spectral features, but matrix photolysis brought about the most distinct changes in the spectra.

Hartree–Fock (HF) calculations were performed on potential product molecules using the Gaussian 94 program package.<sup>8</sup> A Møller–Plesset correlation energy correction followed each calculation and was truncated at second order (MP2 method).<sup>9</sup> The program used the Dunning/Huzinaga full double-zeta basis set with one single first polarization function (D95\*) for each atom.<sup>10</sup> The geometry optimizations used redundant internal coordinates and converged via the Berny optimization algorithm,<sup>8,11</sup> and the program calculated vibrational frequencies analytically.

## Results

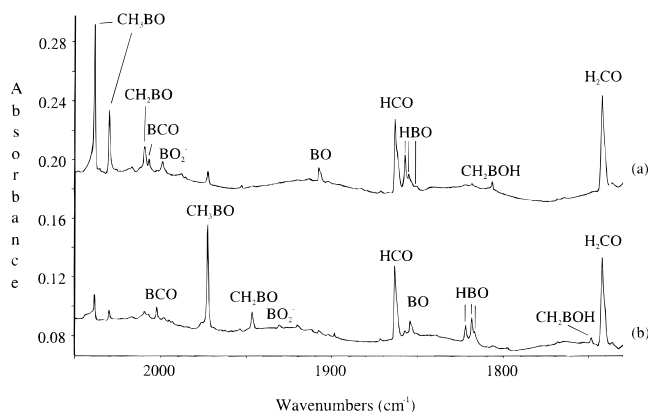
Infrared spectra of the reaction products using various isotopic combinations are reported. The relative increase or decrease of these peaks upon photolysis and annealing helps to assign peaks of different isotopes to the same product. In <sup>nat</sup>B experiments, 4:1 ratios of peaks help identify <sup>11</sup>B and <sup>10</sup>B counterparts of the same species. Several product peaks exhibit no boron shift and correspond to either precursor absorptions or absorptions of precursor fragments. For example, in experiments with CH<sub>3</sub>OH, absorptions at 1741.9, 1498.2, and 1167.2 cm<sup>-1</sup> indicate the presence of formaldehyde, CH<sub>2</sub>O.<sup>12</sup> The unusually strong CO absorption at 2138.0 cm<sup>-1</sup> arises partly from impurities, but also from CO generated from photolyzed CH<sub>3</sub>OH. Strong HCO absorptions at 1863.3 and 1085.0 cm<sup>-1</sup> (1801.8 and 849.1 cm<sup>-1</sup> for DCO) are also present.<sup>13</sup> Because of oxides on the surface of the boron targets and impurities in the system, the spectra all have traces of BO<sub>2</sub><sup>-</sup> and (BO)<sub>2</sub>.<sup>6,14</sup>

<sup>⊗</sup> Abstract published in *Advance ACS Abstracts*, February 1, 1997.

**TABLE 1: Observed Vibrational Frequencies ( $\text{cm}^{-1}$ ) for Various Isotopic Combinations of Boron–Methanol Reactions**

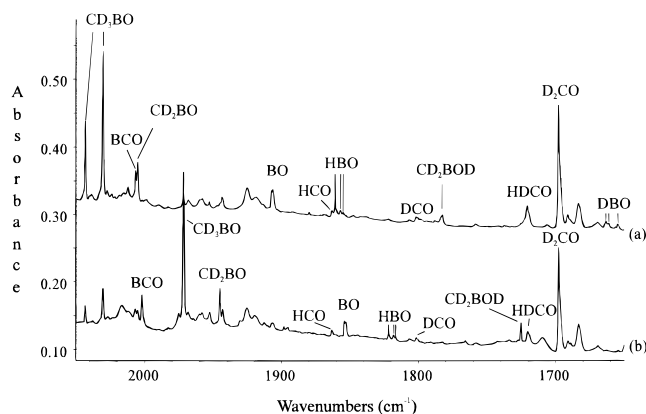
10/1 <sup>a</sup>	11/1 <sup>a</sup>	10/2 <sup>a</sup>	11/2 <sup>a</sup>	photolysis <sup>b</sup>	assignment
2306.9	2298.3		1709.4	+50	(H <sub>2</sub> )BH
2268.3	2259.4			+40	BH
2038.5	1972.4	2030.7	1972.0	+35	CH <sub>3</sub> BO
2029.9 <sup>c</sup>		2043.5 <sup>c</sup>		+35	CH <sub>3</sub> BO
2009.5	1946.6	2005.4	1945.2	+25	CH <sub>2</sub> BO
2006.8	2002.2	2006.8	2002.2	+10	BCO
1907.5	1854.4	1907.5	1854.4	+5	BO
1861.0	1821.9	1663.0	1649.6	+60	HBO
1857.3	1818.4	1660.8	1647.4	+60	HBO site
1855.1	1816.7	1654.3	1641.5	+60	HBO site
1806.5	1748.3	1782.3	1724.9	-100	CH <sub>2</sub> BOH
1449.1	1420.2	1449.1	1420.2	-60	BOB
1305.0	1305.0			+35	CH <sub>3</sub> BO
904.5	896.8	761.0	750.0	+35	CH <sub>3</sub> BO
903.3	895.6			+35	CH <sub>3</sub> BO
765.6	756.7	618.7	607.6	+60	HBO
666.5	663.6	561.4	554.8	+25	CH <sub>2</sub> BO

<sup>a</sup> The first number gives the mass number of the boron isotope, and the second number gives the mass number of the methyl hydrogens. For example, "10/2" represents the results obtained when <sup>10</sup>B reacts with CD<sub>3</sub>OD. <sup>b</sup> Percent change in peak intensity after 45 min of broadband mercury arc photolysis. <sup>c</sup> Fermi resonance splittings (see text).

**Figure 1.** Infrared spectra in the 2050–1730  $\text{cm}^{-1}$  region for laser-ablated boron atoms codeposited with Ar/CH<sub>3</sub>OH samples at 6–7 K. (a) <sup>10</sup>B and (b) <sup>11</sup>B.

**<sup>10</sup>B + CH<sub>3</sub>OH.** Table 1 provides frequencies and photolysis behavior of all isotopic combinations of reaction products. Figure 1a displays a spectrum for the best <sup>10</sup>B experiment in the 2050–1730  $\text{cm}^{-1}$  range. Not shown are bands due to (H<sub>2</sub>)BH at 2306.9  $\text{cm}^{-1}$  and BH at 2268.3  $\text{cm}^{-1}$ .<sup>15</sup> A weak absorption at 2006.8  $\text{cm}^{-1}$  corresponds to BCO,<sup>16</sup> and a BO peak appears at 1907.5  $\text{cm}^{-1}$ .<sup>14,16</sup> Also, just to the red of the 1863.3  $\text{cm}^{-1}$  HCO absorption lie HBO absorption sites at 1861.0, 1857.3, and 1855.1  $\text{cm}^{-1}$ . Although BCO, BO and HBO are often observed in boron experiments,<sup>4,6</sup> the unusually large intensities of these peaks in these experiments indicate that the boron–methanol reactions are the main source of these molecules in the spectra.

The major product bands are at 2038.5 and 2029.9  $\text{cm}^{-1}$ , and both bands increase approximately 35% on photolysis. A weaker band at 2009.5  $\text{cm}^{-1}$  to the blue of BCO increases approximately 25% on photolysis. Just lower in frequency in the carbonyl stretching region, a formaldehyde absorption dominates the spectrum. A smaller peak at 1806.5  $\text{cm}^{-1}$  vanishes upon photolysis and indicates a new highly reactive product. No other new absorptions arise in the 2150–1700  $\text{cm}^{-1}$  region, indicating that there are only a few products with B–O or C–O multiple bonds.

**Figure 2.** Infrared spectra in the 2050–1650  $\text{cm}^{-1}$  region for laser-ablated boron atoms codeposited with Ar/CD<sub>3</sub>OD(H) samples at 6–7 K. (a) <sup>10</sup>B and (b) <sup>11</sup>B.

In the bending region, several new peaks arise and are listed in Table 1. Besides a strong HBO absorption at 765.7  $\text{cm}^{-1}$  and a BOB absorption at 1449.1  $\text{cm}^{-1}$ ,<sup>6</sup> a strong doublet at 904.5, 903.3  $\text{cm}^{-1}$  increases 35% upon photolysis, and a smaller absorption at 666.5  $\text{cm}^{-1}$  increases 25% on photolysis. A weak CH<sub>3</sub> radical band<sup>17</sup> was detected near 610  $\text{cm}^{-1}$ .

**<sup>nat</sup>B + CH<sub>3</sub>OH.** Figure 1b presents the best spectrum for reactions of natural boron with methanol. As for <sup>10</sup>B, modest absorptions due to (H<sub>2</sub>)BH, BH, BCO, and BO are present but shifted. The strongest absorption in the spectrum is at 1972.4  $\text{cm}^{-1}$  and seemingly has its natural <sup>10</sup>B counterpart at 2038.5  $\text{cm}^{-1}$ . A weaker absorption at 1946.6  $\text{cm}^{-1}$  corresponds well with the <sup>10</sup>B absorption at 2009.5  $\text{cm}^{-1}$ . An absorption at 2029.9  $\text{cm}^{-1}$  is much weaker than in the <sup>10</sup>B experiments but does not have any apparent <sup>11</sup>B counterpart in this spectrum with the 1946.6  $\text{cm}^{-1}$  peak shifted too much to be a boron isotopic counterpart. As in the <sup>10</sup>B experiments, HBO is also a major product. Near the CH<sub>2</sub>O absorption, there is a new small peak at 1748.3  $\text{cm}^{-1}$  which vanishes upon photolysis and makes assignment of the 1748.3 and 1806.5  $\text{cm}^{-1}$  peaks as boron isotopic counterparts definitive.

In the bending region, the doublet from the <sup>10</sup>B experiment at 904.5, 903.3  $\text{cm}^{-1}$  reappears with another doublet of 4 times the intensity at 896.8, 895.6  $\text{cm}^{-1}$ , and both increase 35% upon photolysis. An absorption at 663.6  $\text{cm}^{-1}$  appears with a <sup>10</sup>B counterpart at 666.5  $\text{cm}^{-1}$ . The isotopic shift of these two peaks confirms that these bands are not among the CO<sub>2</sub> absorptions in this spectral region.

**<sup>11</sup>B + CH<sub>3</sub>OH.** Experiments with <sup>11</sup>B and CH<sub>3</sub>OH help to confirm the observations made in the <sup>nat</sup>B and <sup>10</sup>B experiments. New peaks assigned to <sup>10</sup>B products did not appear, and all those assigned to <sup>11</sup>B products appeared. The most interesting finding of these experiments is that the 2029.9  $\text{cm}^{-1}$  peak disappeared and, therefore, must arise from a <sup>10</sup>B product despite no obvious <sup>11</sup>B counterpart. Solely on the basis of the <sup>nat</sup>B and <sup>10</sup>B experiments, one could conclude that this absorption was caused by a product lacking boron and that Figure 1b represented an experiment that produced a smaller yield of this product. The <sup>11</sup>B experiments refute that hypothesis and clearly show that the peak at 2029.9  $\text{cm}^{-1}$  is an absorption of a product containing <sup>10</sup>B.

**<sup>10</sup>B + CD<sub>3</sub>OD.** The best spectrum of the products of the reaction of <sup>10</sup>B with CD<sub>3</sub>OD is presented in Figure 2a. Peaks due to BO and BCO, the production of which does not depend upon deuteration of the starting material, remain prominent. The dominant absorption occurs at 2030.7  $\text{cm}^{-1}$  with a nearby strong absorption at 2043.5  $\text{cm}^{-1}$ . Both of these absorptions increase 35% upon photolysis. To the red of the BCO peak is a

**TABLE 2: MP2 Calculations on the Energies, Structures, and Selected Vibrational Frequencies (in  $\text{cm}^{-1}$ ) with Intensities ( $\text{km/mol}$ ) for Potential Products of the Boron–Methanol Reactions**

product (state) <sup>a</sup>	energy (au)	bond lengths ( $\text{\AA}$ )	bond angles (deg)	vib freq (int)
CH <sub>3</sub> BO (S)	-139.251 16	$r_{\text{CH}} = 1.10, r_{\text{CB}} = 1.54, r_{\text{BO}} = 1.23$	$\angle_{\text{HCB}} = 110.3, \angle_{\text{HCH}} = 108.6, \angle_{\text{CBO}} = 180.0$	2014.1 (131), 1394.2 (23), 961.7 ( $2 \times 24$ ), 831.9 (~0)
CH <sub>2</sub> BOH (S)	-139.171 90	$r_{\text{CH}} = 1.09, r_{\text{CB}} = 1.40, r_{\text{BO}} = 1.33, r_{\text{OH}} = 0.97$	$\angle_{\text{HCB}} = 121.4, \angle_{\text{HCH}} = 117.1, \angle_{\text{CBO}} = 180.0, \angle_{\text{BOH}} = 113.9$	3796.4 (168), 1824.1 (370), 1044.4 (195), 629.9 (118), 629.7 (107)
CH <sub>3</sub> OB (S)	-139.144 75	$r_{\text{CH}} = 1.09, r_{\text{CB}} = 1.44, r_{\text{OB}} = 1.31$	$\angle_{\text{HCO}} = 107.0, 109.0, \angle_{\text{HCH}} = 110.5, \angle_{\text{COB}} = 141.7$	1580.0 (213), 1456.7 (269), 921.4 (35)
CH(BH)OH (S)	-139.079 35	$r_{\text{CH}} = 1.10, r_{\text{CB}} = 1.41, r_{\text{BH}} = 1.17, r_{\text{CO}} = 1.40, r_{\text{OH}} = 0.97$	$\angle_{\text{HCB}} = 117.0, \angle_{\text{BCO}} = 126.1, \angle_{\text{HCO}} = 116.6, \angle_{\text{COH}} = 107.1$	3789.6 (61), 1266.8 (114), 1044.2 (38), 835.4 (47), 696.3 (49)
CH <sub>2</sub> BO (D)	-138.622 36	$r_{\text{CH}} = 1.09, r_{\text{CB}} = 1.51, r_{\text{BO}} = 1.23$	$\angle_{\text{HCB}} = 121.4, \angle_{\text{HCH}} = 117.2, \angle_{\text{CBO}} = 180.0$	2020.4 (163), 922.5 (14), 893.7 (~0), 633.6 (84)
BH <sub>2</sub> CO (D)	-138.565 03	$r_{\text{BH}} = 1.19, r_{\text{BC}} = 1.49, r_{\text{CO}} = 1.17$	$\angle_{\text{HBC}} = 116.1, \angle_{\text{HBH}} = 127.8, \angle_{\text{BCO}} = 180.0$	2814.2 (36), 2109.5 (473)
CHBOH (D)	-138.529 34	$r_{\text{CH}} = 1.08, r_{\text{CB}} = 1.37, r_{\text{BO}} = 1.35, r_{\text{OH}} = 0.97$	$\angle_{\text{HCB}} = 178.4, \angle_{\text{CBO}} = 177.5, \angle_{\text{BOH}} = 116.8$	3861.2 (221), 3447.1 (64), 1891.0 (428), 904.3 (272)
CH <sub>2</sub> OB (D)	-138.512 84	$r_{\text{CH}} = 1.08, r_{\text{CO}} = 1.38, r_{\text{OB}} = 1.32$	$\angle_{\text{HCO}} = 113.8, \angle_{\text{HCH}} = 116.2, \angle_{\text{COB}} = 146.3$	1549.7 (260), 1490.5 (212), 1008.2 (17), 589.4 (48)
HBCOH (D)	-138.477 05	$r_{\text{BH}} = 1.17, r_{\text{BC}} = 1.36, r_{\text{CO}} = 1.31, r_{\text{OH}} = 0.98$	$\angle_{\text{HBC}} = 181.7, \angle_{\text{BCO}} = 184.8, \angle_{\text{COH}} = 109.5$	3691.7 (121), 1913.8 (130), 1305.8 (135), 1058.3 (65)
HCBO (T)	-137.989 14	$r_{\text{CH}} = 1.08, r_{\text{CB}} = 1.49, r_{\text{BO}} = 1.23$	$\angle_{\text{HCB}} = 147.0, \angle_{\text{CBO}} = 178.2$	3376.2 (20), 2030.9 (234), 579.2 (2), 447.5 (29)
HBCO (T)	-137.946 91	$r_{\text{BH}} = 1.19, r_{\text{BC}} = 1.41, r_{\text{CO}} = 1.17$	$\angle_{\text{HBC}} = 180.0, \angle_{\text{BCO}} = 180.0$	2059.1 (596), 1120.4 (19)
CBO (T)	-137.348 93	$r_{\text{CB}} = 1.49, r_{\text{BO}} = 1.23$	$\angle_{\text{CBO}} = 180.0$	2033.0 (258), 955.4 (5), 457.0 ( $2 \times 24$ )
BCO (T)	-137.324 89	$r_{\text{BC}} = 1.43, r_{\text{CO}} = 1.18$	$\angle_{\text{BCO}} = 180.0$	2082.6 (744), 1104.1 (4), 496.4 ( $2 \times 3$ )
HBO (D)	-100.183 45	$r_{\text{HB}} = 1.16, r_{\text{BO}} = 1.22$	$\angle_{\text{HBO}} = 180.0$	2995.2 (4), 1810.3 (32) 795.5 (7)
BO (D)	-99.535 61	$r_{\text{BO}} = 1.22$		1919.4 (167)

<sup>a</sup> Ground electronic state abbreviations: S for singlet, D for doublet, T for triplet. <sup>b</sup> Inequivalent bonds.

**TABLE 3: Experimental and Calculated Vibrational Frequencies ( $\text{cm}^{-1}$ ) for CH<sub>3</sub>BO in an Argon Matrix for All Observed Absorptions**

	<sup>10</sup> B/H	<sup>11</sup> B/H	<sup>10</sup> B/D	<sup>11</sup> B/D	B isotopic ratios <sup>a</sup>	H isotopic ratios <sup>b</sup>
obsd	2038.5	1972.4	2030.7	1972.0	1.033 51, 1.029 77	1.003 84, 1.000 20
calcd	2081.0	2014.1	2075.5	2010.3	1.033 22, 1.032 43	1.002 65, 1.001 89
obsd	1305.0	1305.0			1.000 00	
calcd	1394.3	1394.2	1113.2	1113.1	1.000 07, 1.000 09	1.252 52, 1.252 54
obsd	904.5, 903.3	896.8, 895.6	761.0	750.0	1.008 59, <sup>c</sup> 1.014 67	1.187 78, <sup>c</sup> 1.194 93 <sup>c</sup>
calcd	969.6	961.7	808.2	796.6	1.008 21, 1.014 56	1.199 70, 1.207 26

<sup>a</sup> Vibrational frequency ratio of that of the <sup>10</sup>B molecule to that of the <sup>11</sup>B molecule. The first number listed is for CH<sub>3</sub>BO, and the second number is for CD<sub>3</sub>BO. <sup>b</sup> Vibrational frequency ratio of CH<sub>3</sub>BO to CD<sub>3</sub>BO. The first number is for the <sup>10</sup>B molecule, and the second number is for the <sup>11</sup>B molecule. <sup>c</sup> Calculated using the average of the doublet(s).

reasonably strong absorption at 2005.4  $\text{cm}^{-1}$ , which increases 25% upon photolysis. Because approximately 30% of the reactant is CD<sub>3</sub>OH, both HBO and DBO are formed. In the carbonyl region, the only new absorption due to boron reaction occurs at 1782.3  $\text{cm}^{-1}$ , and this vanishes upon photolysis much like the peaks in this region obtained using CH<sub>3</sub>OH. New peaks in the bending region at 761.0  $\text{cm}^{-1}$  (+35% on photolysis) and 561.4  $\text{cm}^{-1}$  (+25%) are observed. The strongest absorption in this region is due to D<sub>2</sub>CO and is much larger than the HDCO absorption. The latter is likely formed by CD<sub>3</sub>OH photodissociation to CDOH, followed by hydrogen migration to carbon.

<sup>nat</sup>B + CD<sub>3</sub>OD(H). The dominant product band in these experiments occurs at 1972.0  $\text{cm}^{-1}$  (Figure 2b). Because this absorption increases upon photolysis by 35%, and because its intensity is approximately 4 times that of the <sup>10</sup>B absorption at 2030.7  $\text{cm}^{-1}$ , these two peaks correspond to isotopic variants of the same species. A smaller absorption at 1945.2  $\text{cm}^{-1}$  matches well with the <sup>10</sup>B peak at 2005.4  $\text{cm}^{-1}$ . As with the CH<sub>3</sub>OH experiments, a <sup>10</sup>B absorption, this time at 2043.5  $\text{cm}^{-1}$ , has no <sup>11</sup>B counterpart.

A <sup>11</sup>B counterpart of the <sup>10</sup>B product absorption at 1782.3  $\text{cm}^{-1}$  can be found at 1724.9  $\text{cm}^{-1}$ , which also vanishes upon photolysis. Corresponding <sup>11</sup>B product bending absorptions can be found at 750.0  $\text{cm}^{-1}$  (corresponding to 761.0  $\text{cm}^{-1}$  for <sup>10</sup>B) and 554.8  $\text{cm}^{-1}$  (561.4  $\text{cm}^{-1}$ ).

**Calculations.** In the boron + methylamine reactions, MP2 calculations played a large role in the identification of product

molecules and radicals,<sup>3</sup> and such calculations help a great deal here. Table 2 presents the results of calculations on potential products of boron–methanol reactions in their ground electronic states. With the exception of HBCO, HCBO, CBO, and BCO, which have triplet ground states, the lowest energy states for all molecules in Table 2 are either singlets or doublets. As with the methylamine studies, the calculated frequencies tend to be higher than the experimental frequencies, but these errors are usually within 10% and are very good when predicting isotopic ratios of vibrational frequencies.

## Discussion

Identification of products makes use of isotopic shifts in vibrational frequency, involving both hydrogen and boron, combined with MP2 calculations of isotopic frequencies.

**Species 1: CH<sub>3</sub>BO.** The dominant absorptions in the B + CH<sub>3</sub>OH reactions occur at 2038.5 and 1972.4  $\text{cm}^{-1}$  for <sup>10</sup>B and <sup>11</sup>B, respectively. As the major product with the lowest calculated energy in Table 2, CH<sub>3</sub>BO should be one of the major products of this reaction, and these two dominant absorptions are assigned to CH<sub>3</sub>BO. MP2 calculations predict these two isotopic modes to appear at 2081.2 and 2014.3  $\text{cm}^{-1}$ , both 2.1% higher than the experimental values. Table 3 lists the experimental and calculated boron isotopic ratios, which are in excellent agreement. The ratio (1.033 51) for this upper band is greater than that of BO (1.028 63), which indicates a mode with boron vibrating between two similar atoms, as in CH<sub>3</sub>BNH.<sup>3</sup>

In the CD<sub>3</sub>OH experiments, the peaks at 2030.7 and 1972.0 cm<sup>-1</sup> correspond to CD<sub>3</sub><sup>10</sup>BO and CD<sub>3</sub><sup>11</sup>BO, respectively. Calculations give frequencies of 2075.7 cm<sup>-1</sup> (+2.2%) and 2010.5 cm<sup>-1</sup> (+2.0%), in good agreement with experiment. The calculated hydrogen isotopic ratios are also near the experimental values (Table 3).

Because of anharmonicity, experimental isotopic ratios tend to be less than calculated harmonic isotopic ratios. Nevertheless, the CH<sub>3</sub>BO boron isotopic ratio and the CH<sub>3</sub><sup>10</sup>BO and CD<sub>3</sub><sup>10</sup>BO hydrogen isotopic ratios exceed their harmonic calculations. For both CH<sub>3</sub>OH and CD<sub>3</sub>OD experiments with <sup>10</sup>B, a peak without an apparent <sup>11</sup>B counterpart appears near the strong CH<sub>3</sub>BO or CD<sub>3</sub>BO bands and behaves exactly the same upon photolysis and matrix annealings to higher temperatures. These bands turn out to be members of Fermi doublets with the strong CH<sub>3</sub><sup>10</sup>BO and CD<sub>3</sub><sup>10</sup>BO absorptions. This band appears to the red of the nominal CH<sub>3</sub>BO absorption and perturbs the major band to higher frequency, which results in a boron isotopic ratio that is higher than expected. For CD<sub>3</sub>BO, the new band appears to the blue of the CD<sub>3</sub>BO fundamental and perturbs it to lower frequency. The combination of these two perturbations increases the observed hydrogen isotopic ratio.

In CH<sub>3</sub>BO, Fermi resonance occurs because of a combination band involving two lower absorptions. For the CH<sub>3</sub>BO molecule with C<sub>3v</sub> symmetry, the 2038.5/1972.4 cm<sup>-1</sup> band (for <sup>10</sup>B/<sup>11</sup>B) represents boron moving between the carbon and oxygen, as in an antisymmetric axial stretch, and has A<sub>1</sub> symmetry. The MP2 calculations predict other bands at 834.2/831.9 cm<sup>-1</sup> (carbon and oxygen moving oppositely with boron nearly stationary, as in a symmetric axial stretching mode) and 1394.3/1394.2 cm<sup>-1</sup> (CH<sub>3</sub> umbrella mode), both of A<sub>1</sub> symmetry. The combination band, then, must also contain A<sub>1</sub> symmetry and be able to couple to the "antisymmetric" stretch. The umbrella mode appears in the spectrum at 1305.0 cm<sup>-1</sup> (calculations predict frequencies 6.8% higher than experiment) for both boron isotopes and increases 35% on photolysis. The 834.2/831.9 cm<sup>-1</sup> band does not appear in the spectrum, but if it is also calculated to be 6.8% too high, then the sum of these two bands would give a harmonic combination band at 2086.1/2083.9 cm<sup>-1</sup> (for <sup>10</sup>B/<sup>11</sup>B), which must be reduced by anharmonicity. Because of the large boron isotopic shift in the "antisymmetric" band and the small isotopic shift in the combination band, the perturbation occurs only for the <sup>10</sup>B isotopic product while the <sup>11</sup>B product spectrum shows no Fermi resonance. For this reason, the 2029.9 cm<sup>-1</sup> absorption is assigned as a combination band of CH<sub>3</sub><sup>10</sup>BO.

For CD<sub>3</sub><sup>10</sup>BO, the situation is similar, except that the source of the Fermi resonance arises from the first overtone of the CD<sub>3</sub> umbrella mode, the fundamental calculated to have <sup>10</sup>B/<sup>11</sup>B frequencies of 1113.2 and 1113.1 cm<sup>-1</sup> for this molecule. Although the dominance of CD<sub>3</sub>OD precursor absorptions in the anticipated spectral region for this peak (near 1040 cm<sup>-1</sup> based upon hydrogen isotopic ratio calculations) prevents its observation, its presence in Figure 2 is certainly evident. The harmonic combination band would be expected to have a frequency near 2080 cm<sup>-1</sup> and, as for CH<sub>3</sub>BO, perturb the <sup>10</sup>B product without affecting the <sup>11</sup>B molecule. For this reason, the 2043.5 cm<sup>-1</sup> peak is assigned as the first overtone of the CD<sub>3</sub> umbrella mode of CD<sub>3</sub>BO.

Based upon the calculations, another mode should be observable in the bending region. Because of the identical photolysis behavior, the two doublets at 904.5, 903.3 cm<sup>-1</sup> and 896.8, 895.6 cm<sup>-1</sup> for <sup>10</sup>B and <sup>11</sup>B, respectively, likely represent this bending mode. Calculations predict this mode at 969.5 cm<sup>-1</sup> (+7.2–7.3%) and 961.6 cm<sup>-1</sup> (+7.2–7.4%). The experimental isotopic

**TABLE 4: Experimental and Calculated Vibrational Frequencies (cm<sup>-1</sup>) for CH<sub>2</sub>BO in an Argon Matrix for All Observed Absorptions. Calculations for HCBO Are Also Provided for Comparison**

	<sup>10</sup> B/H	<sup>11</sup> B/H	<sup>10</sup> B/D	<sup>11</sup> B/D	B isotopic ratios <sup>a</sup>	H isotopic ratios <sup>b</sup>
obsd	2009.5	1946.6	2005.4	1945.2	1.032 31 1.030 95	1.002 04 1.000 72
calcd	2088.2	2020.4	2080.7	2014.6	1.033 56	1.003 60
CH <sub>2</sub> BO					1.032 81	1.002 88
calcd	2099.3	2030.9	2088.8	2022.1	1.033 68	1.005 03
HCBO					1.032 99	1.004 35
obsd	666.5	663.6	561.4	554.8	1.004 37 1.011 90	1.187 21 1.196 11
calcd	637.2	633.6	553.6	544.8	1.005 68	1.151 01
CH <sub>2</sub> BO					1.016 15	1.163 00
calcd	588.4	579.2	542.1	528.5	1.015 88	1.085 41
HCBO					1.025 73	1.095 93

<sup>a</sup> Vibrational frequency ratio of that of the <sup>10</sup>B molecule to that of the <sup>11</sup>B molecule. The top number listed is for CH<sub>2</sub>BO or HCBO, and the bottom number is for CD<sub>2</sub>BO or DCBO. <sup>b</sup> Vibrational frequency ratio of CH<sub>2</sub>BO to CD<sub>2</sub>BO or HCBO to DCBO. The top number is for the <sup>10</sup>B molecule, and the bottom number is for the <sup>11</sup>B molecule.

ratios for both peaks in each doublet agree well with the calculations (Table 3). In the gas phase, this mode is doubly degenerate, but the argon matrix breaks this degeneracy slightly, leading to the observed doublet. For CD<sub>3</sub>BO, no such doublets appear, and the absorptions of this mode are at 761.0 and 750.0 cm<sup>-1</sup>. MP2 calculations for the deuterated molecule give frequencies of 808.2 cm<sup>-1</sup> (+6.2%) and 796.5 cm<sup>-1</sup> (+6.2%), with a boron isotopic ratio in excellent agreement with experiment. If the average of the two peaks in the CH<sub>3</sub>BO doublets is considered, the experimental and calculated hydrogen isotopic ratios are similarly convincing as to these peak assignments.

**Species 2: CH<sub>2</sub>BO.** The bands at 2009.5 and 1946.6 cm<sup>-1</sup> for CH<sub>3</sub>OH experiments belong to boron isotopic variants of the same product. The large boron isotopic ratio, 1.032 31, indicates that boron is vibrating between carbon and oxygen, as in CH<sub>3</sub>BO. Because these peaks shift upon deuteration, the identity of this species must be limited to CH<sub>2</sub>BO or HCBO. Calculations for the former yield frequencies of 2088.2 cm<sup>-1</sup> (+3.9%) and 2020.4 cm<sup>-1</sup> (+3.8%) for <sup>10</sup>B and <sup>11</sup>B and a boron isotopic ratio in very good agreement with experiment, as shown in Table 4. HCBO calculations are nearly as good, with vibrational frequencies calculated at 2099.3 cm<sup>-1</sup> (+4.5%) and 2030.9 cm<sup>-1</sup> (+4.3%). The strongest bending modes are calculated at 637.2/633.6 cm<sup>-1</sup> for CH<sub>2</sub>BO and at 588.4/579.2 cm<sup>-1</sup> for HCBO. Because the spectra give a boron isotopic doublet at 666.5/663.6 cm<sup>-1</sup> that upon photolysis behaves like the 2009.5/1946.6 cm<sup>-1</sup> doublet, both doublets likely belong to the same product, which the evidence suggests is CH<sub>2</sub>BO. The bending mode calculations predict frequencies below those of experiment but are much closer in the case of CH<sub>2</sub>BO than for HCBO, as are the boron isotopic ratios (Table 4). While MP2 calculations rarely underestimate stretching frequencies, they occasionally do so for bending frequencies, especially in open-shell systems.

For the deuterated experiments, the peaks at 2005.4 and 1945.2 cm<sup>-1</sup> correspond to CD<sub>2</sub><sup>10</sup>BO and CD<sub>2</sub><sup>11</sup>BO, respectively. MP2 calculations predict frequencies at 2080.7 cm<sup>-1</sup> (+3.8%) and 2014.6 cm<sup>-1</sup> (+3.6%). The predicted hydrogen isotopic ratios are sufficiently close to experiment to confirm the identification of this open-shell radical (Table 4). The calculated frequencies for the bending mode of the deuterated product agree very well with observed peaks at 561.4 cm<sup>-1</sup> (calculations are 1.4% too low) and 554.8 cm<sup>-1</sup> (-1.8%).

**Species 3: CH<sub>2</sub>BOH.** The peaks at 1806.5 and 1748.3 cm<sup>-1</sup> belong to CH<sub>2</sub>BOH. Although this is a structural isomer of species 1, MP2 calculations predict this molecule to be 50 kcal/mol less stable. For this reason, the absorptions are weak despite strong predicted oscillator strengths (Table 2). Also, because the concentration of this product is quite small, none of the other absorptions, all calculated to be weaker than the present peak, can be seen. Photolysis destroys CH<sub>2</sub>BOH and probably converts this molecule into CH<sub>3</sub>BO by rearrangement or into CH<sub>2</sub>BO by loss of the methoxy hydrogen. Calculations predict these frequencies at 1887.8 cm<sup>-1</sup> (+4.5%) and 1824.1 cm<sup>-1</sup> (+4.3%).

For the deuterated experiments, peaks at 1782.3 and 1724.9 cm<sup>-1</sup> vanish following mercury arc photolysis and are assigned to CD<sub>2</sub>BOD. Because much of the reactant molecule was CD<sub>3</sub>OH, the presence of CD<sub>2</sub>BOH would be expected. Calculations on CD<sub>2</sub>BOD predict frequencies of 1860.3 cm<sup>-1</sup> (+4.4%) and 1798.3 cm<sup>-1</sup> (+4.3%) while for CD<sub>2</sub>BOH these values are 1864.7 and 1802.7 cm<sup>-1</sup> for <sup>10</sup>B and <sup>11</sup>B, respectively. There are no CD<sub>2</sub>BOH absorptions near in frequency to those of CD<sub>2</sub>BOD that also vanish upon photolysis; this suggests that the original methoxy hydrogen is eliminated, and a methyl hydrogen migrates to the oxygen. Even in experiments with more CD<sub>3</sub>OH than CD<sub>3</sub>OD, no evidence for CD<sub>2</sub>BOH exists. The predicted hydrogen isotopic ratios for CD<sub>2</sub>BOD, 1.014 78 and 1.014 35, closely match the experimental values of 1.013 58 and 1.013 57 for <sup>10</sup>B and <sup>11</sup>B, respectively.

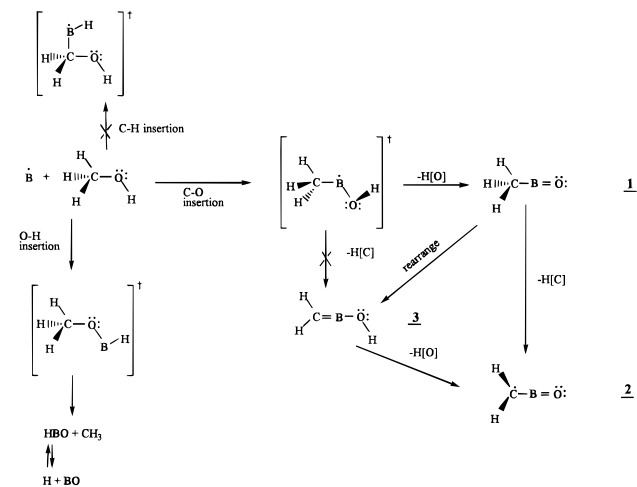
**Reaction Mechanisms.** The basic boron insertion reaction mechanisms closely resemble those of the boron–methylamine reactions, where excess kinetic energy<sup>13</sup> in the laser-ablated boron atoms activates after the insertion reactions. As with methylamine, there are three types of bonds in which boron may insert: a C–H bond, a C–O bond, and an O–H bond. Following insertion, dehydrogenation and C–O bond breaking produce the products observed in the spectrum. Calculations on the insertion products show that insertion into the C–O bond is exoergic by 107 kcal/mol and insertion into the O–H bond is exoergic by 87 kcal/mol. By contrast, insertion into the C–H bond is only 49 kcal/mol exoergic, and the only products observed potentially from C–H insertion are BH, BCO, and H<sub>2</sub>CO. Alternatively, BCO can be formed entirely by photolytic generation of CO from CH<sub>3</sub>OH in the laser plume followed by association with B atoms, BH can be formed by union of dissociated H and B, and H<sub>2</sub>CO is likely a photolysis product. These alternatives suggest that C–H insertion is not required for the observable products in boron–methanol experiments.

Insertion into C–O provides for all of the new products observed here. Loss of a single hydrogen would generate CH<sub>3</sub>BO or CH<sub>2</sub>BOH, with the former much more thermodynamically favored. The CD<sub>3</sub>OD/CD<sub>3</sub>OH experiments reveal that formation of CH<sub>2</sub>BOH results from elimination of the methoxy hydrogen and probably occurs via rearrangement of CH<sub>3</sub>BO prior to relaxation in the argon matrix. From either CH<sub>3</sub>BO or CH<sub>2</sub>BOH, further loss of a single hydrogen can generate CH<sub>2</sub>BO. No spectroscopic evidence was found for other products like HCBO.

Insertion into O–H must usually be followed by breaking of the C–O bond to form CH<sub>3</sub> and HBO, but these products are very weak. Otherwise, formation of CH<sub>3</sub>OB might be expected, and there is no experimental evidence for the presence of this molecule. HBO may further degrade to H and BO. Scheme I diagrams the pathways for the various products observed in boron–methanol reactions.

**Bonding.** The main evidence that iminoboranes contain a B–N triple bond is the calculated geometry, which indicates

## SCHEME 1



that the R–B–N and B–N–R bond angles were 180°. For CH<sub>3</sub>BO and CH<sub>2</sub>BO, the calculated C–B–O bond angles are 180°, but such a geometry is consistent with both double and triple B–O bonding (i.e., both no formal charge separation and full formal charge separation). For CH<sub>2</sub>BOH, however, the B–O–H bond angle reveals quite a bit about the degree of bonding. Because the C–B bond is a double bond, the B–O bond would have to be a single bond if neither oxygen lone pair bonded to boron, and the oxygen would be sp<sup>3</sup> hybridized with a B–O–H bond angle near 109°. If this bond angle approaches 120°, however, sp<sup>2</sup> hybridization is suggested with oxygen donating a lone pair to covalent bonding with boron and accepting a formal positive charge. According to the results in Table 2, the B–O–H bond angle is 114° and suggests that some degree of B–O multiple bonding exists in CH<sub>2</sub>BOH, but not to the full extent as in the analogous molecule CH<sub>3</sub>BNH.<sup>3</sup> One might expect, then, that the B–O bond in CH<sub>3</sub>BO has partial triple bond character, and because the calculated B–O distance is virtually the same, the B–O bonds in CH<sub>2</sub>BO and HBO also have some triple bond character.

## Conclusions

The reaction of laser-ablated boron atoms with methanol yields three major new species, CH<sub>3</sub>BO, CH<sub>2</sub>BO, and CH<sub>2</sub>BOH, when the products are isolated in an argon matrix. Each of these major products follows boron insertion into the C–O bond and subsequent dehydrogenation. Another product of this reaction, HBO, forms following boron insertion into the O–H bond and subsequent C–O bond cleavage. Although there are 3 times as many C–H bonds, no products resulting from insertion into the methyl group are observed. As with reactions of boron and methylamine, the C–H bond is simply too strong, and breaking this bond to form products is more difficult when compared to more energetically favorable alternatives. The resulting major products all have B–O bonds, each with at least some multiple bond character caused by an oxygen atom lone pair coordinating with the empty boron p-orbital.

**Acknowledgment.** We gratefully acknowledge support for this research from the Air Force Office of Scientific Research and computer time from the San Diego Supercomputer Center.

## References and Notes

- (1) Thompson, C. A.; Andrews, L. *J. Am. Chem. Soc.* **1995**, *117*, 10125.
- (2) Thompson, C. A.; Andrews, L.; Martin, J. M. L.; El-Yazal, J. *J. Phys. Chem.* **1995**, *99*, 13839.
- (3) Lanzisera, D. V.; Andrews, L. *J. Phys. Chem. A* **1997**, *101*, 824.

- (4) Hassanzadeh, P.; Andrews, L. *J. Am. Chem. Soc.* **1992**, *114*, 9239.
- (5) Hassanzadeh, P.; Hannachi, Y.; Andrews, L. *J. Phys. Chem.* **1993**, *97*, 6418.
- (6) Andrews, L.; Burkholder, T. R. *J. Phys. Chem.* **1991**, *95*, 8554.
- (7) Hassanzadeh, P.; Andrews, L. *J. Phys. Chem.* **1992**, *96*, 9177.
- (8) Gaussian 94, Revision B.1: Frisch, M. J.; Trucks, G. W.; Schlegel, H. B.; Gill, P. M. W.; Johnson, B. G.; Robb, M. A.; Cheeseman, J. R.; Keith, T.; Petersson, G. A.; Montgomery, J. A.; Raghavachari, K.; Al-Laham, M. A.; Zakrzewski, V. G.; Ortiz, J. V.; Foresman, J. B.; Cioslowski, J.; Stefanov, B. B.; Nanayakkara, A.; Challacombe, M.; Peng, C. Y.; Ayala, P. Y.; Chen, W.; Wong, M. W.; Andres, J. L.; Replogle, E. S.; Gomperts, R.; Martin, R. L.; Fox, D. J.; Binkley, J. S.; Defrees, D. J.; Baker, J.; Stewart, J. P.; Head-Gordon, M.; Gonzalez, C.; Pople, J. A. Gaussian, Inc., Pittsburgh, PA, 1995.
- (9) Head-Gordon, M.; Pople, J. A.; Frisch, M. J. *Chem. Phys. Lett.* **1988**, *153*, 503. Frisch, M. J.; Head-Gordon, M.; Pople, J. A. *Chem. Phys. Lett.* **1990**, *166*, 275. Frisch, M. J.; Head-Gordon, M.; Pople, J. A. *Chem. Phys. Lett.* **1990**, *166*, 281.
- (10) Dunning, T. H., Jr.; Hay, P. J. In *Modern Theoretical Chemistry*; Schaefer, H. G. III, Ed.; Plenum: New York, 1976; pp 1–28.
- (11) Schlegel, H. B. *J. Comput. Chem.* **1982**, *3*, 214.
- (12) Nelander, B. *J. Chem. Phys.* **1980**, *72*, 77. Andrews, L.; Johnson, G. L. *J. Phys. Chem.* **1984**, *88*, 5887.
- (13) Milligan, D. E.; Jacox, M. E. *J. Chem. Phys.* **1971**, *54*, 927.
- (14) Burkholder, T. R.; Andrews, L. *J. Chem. Phys.* **1991**, *95*, 8697.
- (15) Tague, T. J., Jr.; Andrews, L. *J. Am. Chem. Soc.* **1994**, *116*, 4970.
- (16) Burkholder, T. R.; Andrews, L. *J. Phys. Chem.* **1992**, *96*, 10195.
- (17) Milligan, D. E.; Jacox, M. E. *J. Chem. Phys.* **1967**, *47*, 5146.